

# Competing collinear and noncollinear interactions in chirped quasi-phase-matched optical parametric amplifiers

Mathieu Charbonneau-Lefort,<sup>1,\*</sup> Bedros Afeyan,<sup>2</sup> and M. M. Fejer<sup>1</sup>

<sup>1</sup>*E. L. Ginzton Laboratory, Stanford University, Stanford, California 94305, USA*

<sup>2</sup>*Polymath Research Inc., Pleasanton, California 94566, USA*

\*Corresponding author: *mathieu@polymath-usa.com*

Received April 2, 2008; revised June 24, 2008; accepted July 1, 2008;  
posted July 7, 2008 (Doc. ID 94433); published August 5, 2008

Chirped quasi-phase-matched optical parametric amplifiers (chirped QPM OPAs) are investigated experimentally. The measured collinear gain is constant over a broad bandwidth, which makes these devices attractive candidates for use in femtosecond amplifier systems. The experiment also shows that chirped QPM OPAs support noncollinear gain-guided modes. These modes can dominate the desired collinear gain and generate intense parametric fluorescence. Design guidelines to mitigate these parasitic processes are discussed. © 2008 Optical Society of America

OCIS codes: 140.4480, 190.4970, 190.4410, 190.7110, 320.1590, 320.5540.

## 1. INTRODUCTION

Optical amplifiers are an essential component of high-power ultrafast laser systems [1,2]. Typically, amplification from the nanojoule up to the millijoule level and beyond is realized using the chirped-pulse amplification (CPA) technique [3]. In these systems the amplification is traditionally carried out by solid-state optical amplifiers. An alternative approach is to use optical parametric amplifiers (OPAs) [4–6]. Among the advantages of OPAs is that they allow the choice of amplification wavelength, offer large single-pass gains, are less affected by thermal effects, and offer reduced prepulsing.

For femtosecond pulse amplification it is often necessary to broaden the bandwidth of OPAs. A straightforward way of achieving this is to operate near degeneracy (i.e., choose approximately equal signal and idler wavelengths) [7]. Another approach is to use a noncollinear geometry [8–10]. Recently, it has been proposed to achieve broadband optical parametric amplification using *chirped* quasi-phase matched (QPM) gratings [11–14].

The quasi-phase-matching technique involves the engineering of the nonlinear optical material in order to ensure phase matching at desired wavelengths [15]. In common ferroelectrics such as lithium niobate, it is implemented by a periodic reversal of the sign of the nonlinear susceptibility through periodic reversals of the orientation of ferroelectric domains. One of the advantages offered by this technique is the ability to realize nonuniform, or chirped, phase-matching profiles. In principle, chirped QPM OPAs offer arbitrarily large bandwidths and enable shaping of the gain and group-delay spectra [12–14].

Our initial experiments with chirped QPM OPAs revealed the existence of unexpected high-gain parametric processes in addition to the intended collinear process. These observations lead to the formulation of a 2D model

including noncollinear propagation, diffraction, and transverse localization of the pump beam. Numerical and analytical results have been presented in [16]. Here we report the experimental investigation of the competing processes existing in chirped QPM OPAs and guidelines for evading these undesired effects.

The simplest amplification mechanism is provided by the collinear gain. It is the desired behavior of the amplifier. In a collinear geometry and in a nonuniform phase-matching medium the amplification is limited to the vicinity of the phase-matching point. In the case of linearly chirped profiles this gain is essentially constant over a broad spectrum. This property makes chirped QPM gratings attractive candidates for applications such as femtosecond-pulse amplifiers. The collinear gain can be described by a 1D model, as detailed in [13,14], and is reviewed in Subsection 2.A. Measurements are presented in Section 4.

Noncollinear parametric interactions compete with the collinear gain. Whether they are seeded by the input signal or by spontaneous fluorescence, they are usually undesired because they can dominate the useful collinear gain of the amplifier. The experimental investigation of these processes is reported in Sections 5 and 6. Finally, design guidelines for the suppression of competing noncollinear modes are discussed in Section 7.

## 2. OVERVIEW OF COLLINEAR AND NONCOLLINEAR PARAMETRIC PROCESSES IN CHIRPED QUASI-PHASE-MATCHED

### A. Collinear Gain

We consider three waves—the pump, signal, and idler—satisfying the energy-conservation condition  $\omega_p = \omega_s + \omega_i$ . Consequently, any detuning  $\delta\omega$  of the signal frequency is accompanied by a shift of the idler frequency by an

amount  $-\delta\omega$ . Here we assume that the spectral bandwidth of the pump is narrow enough that it can be treated as monochromatic.

The wave-vector mismatch of a collinear optical parametric interaction in a QPM grating is given by  $\kappa = k_p - k_s - k_i - K_g$ , where  $k_p$ ,  $k_s$ , and  $k_i$  are the pump, signal, and idler wave vectors, and  $K_g = 2\pi/\Lambda_g$  is the wave vector associated with the grating ( $\Lambda_g$  being the period of the QPM grating). Let  $\lambda_{s0}$  and  $\lambda_{i0}$  be the nominal signal and idler wavelengths. Neglecting higher-order dispersion, the  $k$  vectors can be expanded around those values:  $k_s \approx k_{s,i0} \pm \partial k / \partial \omega|_{k,i0} \delta\omega = k_{s,i0} \pm v_s \delta\omega_{s,i}$ , where  $v_s$  and  $v_i$  are the signal and idler group velocities, respectively. In the following, we will assume that this lowest-order expansion is valid and that medium anisotropy can be ignored.

Although many realistic designs will involve nonlinear QPM grating profiles, the essential features of chirped QPM OPAs are captured by the simple linear profile. In the case of linearly chirped QPM gratings, the grating wave vector can be expressed as  $K_g(z) = K_{g0} - \kappa'(z - z_{pm0})$ , where  $\kappa'$  is the chirp rate and  $z$  is the direction of propagation. The value of  $K_{g0}$  is chosen to ensure phase matching at the nominal wavelengths:  $K_{g0} = k_p - k_{s0} - k_{i0}$ . In this case, the wave-vector mismatch becomes

$$\kappa = \kappa'(z - z_{pm}), \quad (1)$$

where

$$z_{pm} = z_{pm0} + \frac{(1/v_s - 1/v_i)\delta\omega}{\kappa'}, \quad (2)$$

is the position of the perfect phase-match point (PPMP), which varies linearly with frequency detuning.

The three waves interact as they propagate through the nonlinear optical crystal. The strength of the interaction is given by the coupling coefficient,

$$\gamma_0 = \sqrt{\frac{\omega_s \omega_i}{n_s n_i} \frac{d_{\text{eff}}}{c} |E_p|}. \quad (3)$$

In this expression  $\omega_{s,i}$  and  $n_{s,i}$  are the signal and idler frequencies and refractive indices, respectively;  $d_{\text{eff}}$  is the effective nonlinear coefficient of the QPM grating;  $c$  is the speed of light; and  $|E_p|$  is the magnitude of the pump wave electric field.

Collinear parametric interactions in linearly nonuniform phase-matching media in the absence of pump depletion are described approximately by the Rosenbluth model [13,17]. According to this model, the signal and idler experience amplification over a region of width  $4\gamma_0/|\kappa'|$  centered around the PPMP. The (power) gain is given by the Rosenbluth gain formula

$$G_R = \exp\left(\frac{2\pi\gamma_0^2}{|\kappa'|}\right). \quad (4)$$

The logarithmic gain of a chirped QPM grating is therefore proportional to the *intensity* of the pump beam and inversely proportional to the chirp rate. It is convenient to introduce the gain parameter,  $\lambda_R \equiv \gamma_0^2/|\kappa'|$ . Then, the Rosenbluth gain formula is simply  $G_R = \exp(2\pi\lambda_R)$ .

By comparison, the power gain of a uniform QPM grating is  $\frac{1}{4}\exp(2\gamma_0 L)$ , where  $L$  is the length of the grating. In this case the logarithmic gain is proportional to the *amplitude* of the electric field of the pump beam.

This simple expression, Eq. (4), neglects the abrupt turn-on and -off of the interaction at the ends of the QPM grating. The complete result has significant ripples in the amplitude of the gain and the group delay within the pass band of the amplifier, which are not reproduced in the Rosenbluth formula. These ripples can be eliminated by apodizing the QPM grating [13,18].

We define  $\Delta K_g \equiv K_{g,\text{max}} - K_{g,\text{min}}$ , the range of wave vectors contained inside the QPM grating. In the case of a linearly chirped grating,  $\Delta K_g = |\kappa'|L$ . This range determines the bandwidth of the amplifier. If we ignore group-velocity dispersion, the amplification bandwidth is

$$\Delta\omega = \frac{\Delta K_g}{|1/v_s - 1/v_i|}. \quad (5)$$

Inside this bandwidth the average gain is given by Eq. (4).

For extremely broadband OPAs the factor  $\omega_s \omega_i$  in Eq. (3) leads to frequency dependence of the gain, as can the higher-order dispersion neglected in these expressions. Flat gain spectra over broad bandwidths can be obtained through the use of a nonlinearly chirped QPM grating [12].

The desired performance of the amplifier (i.e., gain and bandwidth) determines the required gain parameter,  $\lambda_R$ , and phase-matching range,  $\Delta K_g$ . This leaves the coupling coefficient,  $\gamma_0$ , and the grating length,  $L$ , as free parameters. For a fixed gain and bandwidth the required strength of the pump beam is related to the amplifier length by

$$\gamma_0 = \sqrt{\frac{\lambda_R \Delta K_g}{L}}. \quad (6)$$

## B. Noncollinear Phase Matching

We now consider the more general case of noncollinear interactions. Figure 1 illustrates the geometry. In this case, the phase-matching condition is  $\mathbf{k}_p - \mathbf{k}_s - \mathbf{k}_i - \mathbf{K}_g = 0$ . We assume that the pump and grating wave vectors are collinear and coincide with the  $z$  axis. Let  $\theta_s$  and  $\theta_i$  be the noncollinear angles between the signal and idler wave vectors and that of the pump. We assume that the signal and idler wavelengths are fixed.

As before, we define the (collinear) wave-vector mismatch,  $\kappa(\omega_s, z) = k_p - k_s - k_i - K_g(z)$ . We denote  $z_{pm0}$ , the position of the collinear PPMP at the reference frequency, i.e., such that  $\kappa(\omega_{s0}, z_{pm0}) = 0$ .

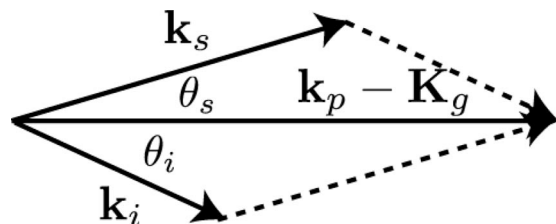


Fig. 1. Noncollinear phase-matching.

In the small-angle approximation the phase-matching angles are

$$\theta_s(\omega_s, z) = \sqrt{\frac{-2\kappa(\omega_s, z)}{k_s(1 + k_s/k_i)}}, \quad (7)$$

and  $\theta_i = -(k_s/k_i)\theta_s$ , where  $k_s = \omega_s n_s/c$  and  $k_i = \omega_i n_i/c$ . The angles have opposite signs, meaning that the signal and idler waves propagate away from the pump beam and in opposite directions.

In the case of a linearly chirped QPM grating the wave-vector mismatch is  $\kappa(\omega_s, z) = \kappa'(z - z_{pm0})$ . If the chirp rate  $\kappa'$  is negative, then noncollinear phase matching is possible for  $z > z_{pm0}$ . On the other hand, if the chirp rate is positive, then noncollinear phase matching is possible only for  $z < z_{pm0}$ .

### C. Noncollinear Gain-Guided Modes

We now turn our attention to noncollinear interactions in the presence of a *laterally localized* pump beam. If the QPM grating was uniform, then gain-guided signal and idler modes would exist provided that the gain is large enough to balance the energy loss caused by the propagation of waves away from the interaction region. These modes have been studied in the context of laser-plasma interactions by Suschik and Freidman [19].

Recently, it has been shown that noncollinear gain-guided modes can also exist in *non-uniform* media [16]. The noncollinear angle must be large enough so that the signal and idler waves leave the amplification region before experiencing significant dephasing. If the angle is too small then dephasing caused by the nonuniform phase-matching profile suppresses the existence of gain-guided modes. In this regime the amplification is described adequately by the Rosenbluth model because significant growth is limited to the vicinity of the phase-matched point. On the other hand, if the angle is too large then the gain is insufficient to ensure gain guiding. For a range of phase-matching angles between these limits noncollinear processes with significant gain exist.

Figure 2 shows a plot of the growth rate of noncollinear gain-guided modes as a function of angle for a variety of chirp rates. This graph was obtained numerically as described in [16], assuming only one transverse dimension,  $x$ , and a Gaussian pump profile,  $\exp(x/w_0)^2$ , with  $w_0$  being the half-width of the pump beam. The wavelengths are those used in the experiment described in Section 6 ( $\lambda_i \approx 2.1\lambda_s$ ), corresponding to the asymmetric configuration  $\theta_i \approx 2.1\theta_s$ .

Figure 3 illustrates the amplification of noncollinear interactions in chirped QPM gratings. A signal wave with incidence angle  $\theta_{inc}$  is first amplified at the PPMP,  $z_{pm}$ . If the angle is small the wave only sees the collinear gain given by the Rosenbluth gain formula, Eq. (4). However, at larger angles noncollinear gain-guided modes can be excited, with an angle-dependent growth rate  $K(\theta_{inc})$ . The carrier wave vector of this mode then varies continuously in  $z$  in order to satisfy local noncollinear phase matching. If the chirp rate is negative, the gain length of these modes is limited only by the length of the medium. On the other hand, if the chirp rate is positive, then gain-guided modes will grow until they reach the collinear PPMP,

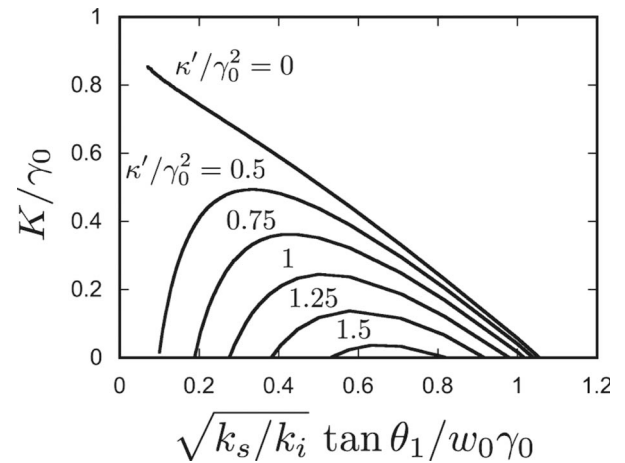


Fig. 2. Normalized growth rate,  $K/\gamma_0$ , as a function of normalized angle,  $\sqrt{k_s/k_i} \tan \theta_1 / w_0 \gamma_0$ , where  $w_0$  is the half-width of the pump beam, for various values of the inverse Rosenbluth gain parameter  $\kappa'/\gamma_0^2 = 1/\lambda_R$ . This plot was obtained numerically as described in [16] assuming a single transverse dimension and a Gaussian pump profile, for the case  $\theta_i \approx 2.1\theta_s$  corresponding to the experiment.

$z_{pm0}$ , after which it becomes impossible to phase-match the interaction. Although finite, this gain length can be much longer than the Rosenbluth amplification region, and as a consequence the gain of noncollinear interactions is often much larger than the collinear gain. This explains why gain-guided modes affect the design of chirped QPM OPAs.

Parasitic noncollinear processes can take place even when the input signal is collinear with the pump. Spontaneous emission can seed noncollinear gain-guided modes and give rise to parametric fluorescence. Another mechanism is specific to negatively chirped QPM gratings: if the pump is tightly focused, the signal and idler beams amplified at the PPMP are also very narrow and can contain a large range of spatial frequencies. The frequency components with sufficiently wide angles can in turn seed noncollinear gain-guided modes, which, in the case of QPM gratings with negative chirp rates, can be amplified beyond the collinear PPMP over the remaining length of the crystal. Due to this process chirped QPM OPAs with focused pump beams seeded collinearly behave very differently depending on whether the chirp rate is positive or negative.

In a 2D model such as the one described in [16], there are two degenerate noncollinear modes sharing the same angle. (They correspond to the signal beam incident from either side of the pump beam.) In a 3D geometry, and assuming a cylindrically symmetric pump beam, the direction of degenerate noncollinear modes describes a cone. If all modes are seeded equally, for example by parametric “noise,” then the parametric fluorescence is most intense along the cone defined by the angle of maximum growth rate. In this case the far-field fluorescence pattern has the shape of a ring. Alternatively, one can imagine applications in which a particular mode or set of modes is excited preferably—for instance, by crossing the pump and signal beam—in order to take advantage of the noncollinear gain.

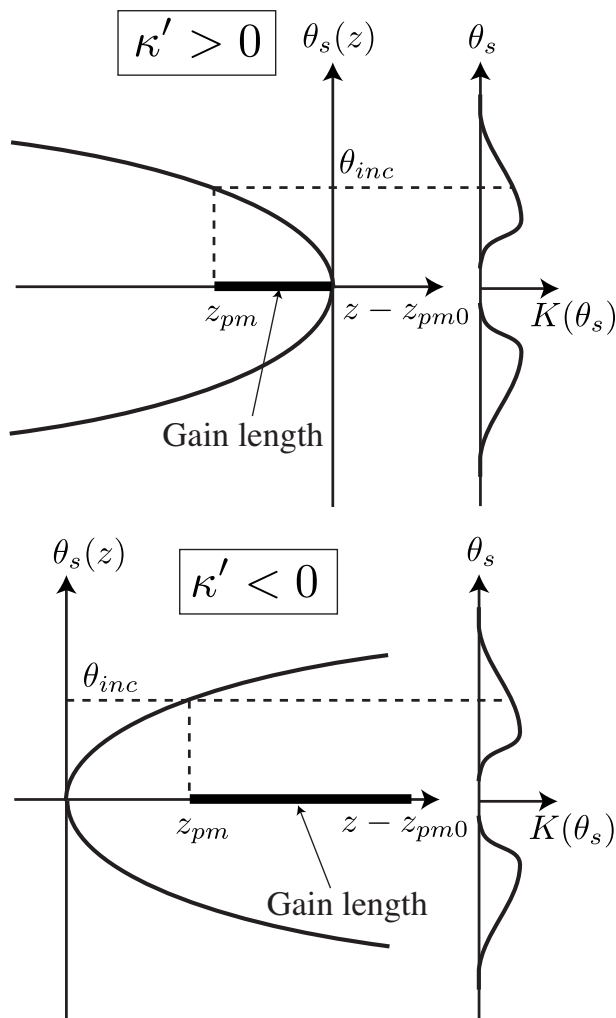


Fig. 3. Illustration of noncollinear interactions in chirped QPM gratings. A signal wave with incidence angle  $\theta_{inc}$  is phase-matched at position  $z_{pm}$ . Depending on the angle a gain-guided mode can be supported, with growth rate  $K(\theta_{inc})$ . This mode grows until the collinear PPMP is reached, in the case of positive chirp rate, or indefinitely in the case of negative chirp rate.

### 3. EXPERIMENTAL SETUP

A diagram of the experimental setup is presented in Fig. 4. The pump laser is a Q-switched Nd:YAG laser from JDS-Uniphase, model Power Chip Nanolaser (1064 nm, 1 kHz repetition rate, 0.8 ns pulse duration, 30  $\mu$ J per pulse). The signal laser is a tunable external-cavity diode laser (ECDL), fabricated by New Focus, model Vidia-Swept (wavelength range from 1500 to 1640 nm, 3 mW of cw power).

The beams are combined and focused inside the nonlinear crystal. The beam waist of both the pump and the signal was 115  $\mu$ m ( $1/e^2$  intensity radius), which corresponds to slightly looser than confocal focusing. The nonlinear crystal consists of periodically poled lithium niobate (PPLN). Each crystal contained several 5 cm long QPM gratings with various chirp rates.

After the nonlinear crystal the pump light is filtered out using a dichroic mirror. Cameras are used to monitor the beam profiles. A slab of silicon after the lithium niobate crystal blocks wavelengths below 1.1  $\mu$ m (such as

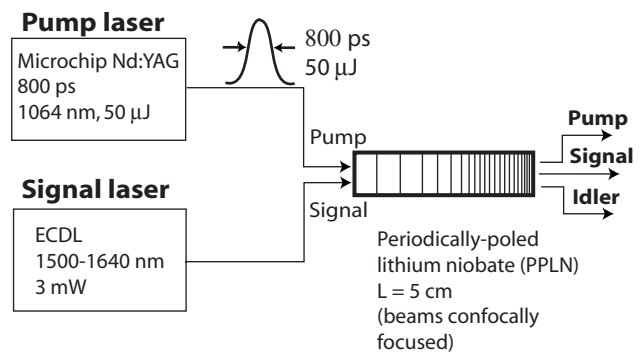


Fig. 4. Experimental setup.

the green light resulting from the parasitic second-harmonic generation of the pump). The output beam (now containing signal and idler wavelengths) is sent through a monochromator. The monochromator is used to filter out the parametric fluorescence. The remaining light is then detected using a Thorlabs InGaAs photodiode, model PDA400 (response time around 30 ns).

A direct measurement of the gain is difficult due to the fact that the increment to the cw seed power due to the OPA with low-duty-cycle pump is small compared to the average seed power. To make gain measurements easier we used a boxcar integrator in order to integrate the electrical signal over the duration of the electrical pulse output from the photodetector.

We observed large pulse-to-pulse variations in the measured gain, due to the exponential dependence of the gain on the pump intensity. To obtain a statistical description of the amplification the electrical signal coming from the boxcar was acquired by a computer. The value quoted for the gain is the mode of a distribution of  $10^4$  pulses.

### 4. MEASUREMENT OF THE COLLINEAR GAIN OF CHIRPED QUASI-PHASE-MATCHED GRATINGS

In this section we present our measurement of the collinear gain. According to the Rosenbluth model reviewed in Subsection 2.A we expect the gain spectrum to be flat over a wide bandwidth.

In this section we consider QPM gratings with a positive chirp rate only. As we recall from the discussion in Subsection 2.C, the Rosenbluth gain of negatively chirped QPM gratings can be dominated by parasitic gain-guided noncollinear modes. Discussion of experimental results for negative chirp rates is given in Section 5.

The amplified signal power was calculated by taking the amplified energy measured by the boxcar integrator,  $U_{\text{amplified}}$ , subtracting the integrated cw seed,  $U_{\text{seed}}$ , and dividing by the duration of the pump beam. The average gain was obtained by dividing the amplified power by the input power

$$G = 1 + \frac{(U_{\text{amplified}} - U_{\text{seed}})/T_{\text{pump}}}{U_{\text{seed}}/T_{\text{int}}}, \quad (8)$$

where  $T_{\text{pump}}=800$  ps is the duration of the pump beam and  $T_{\text{int}}=200$  ns is the integration time.

### A. Gain Spectrum

The gain spectra of three chirped gratings designed to phase match bandwidths of 50, 120, and 190 nm are shown in Fig. 5. They were obtained for a pump pulse energy of  $25 \mu\text{J}$  per pulse. The solid lines are a fit showing the square bandwidths expected from the Rosenbluth model while the solid markers represent experimental data. The measured gain behaves as predicted over the short-wavelength side portion of the spectrum but is completely dominated by parametric fluorescence over the long-wavelength side portion of the spectrum. The gain spectrum of a shorter uniform grating is shown by comparison to illustrate the difference between the bandwidth of uniform and chirped QPM gratings. The large parametric fluorescence observed in this experiment is caused by noncollinear gain-guided modes seeded by parametric noise. These modes will be explored in Section 6.

It is possible to dominate the parametric fluorescence by using a more intense input signal beam. We used an erbium-doped fiber amplifier (EDFA) in order to raise the power of the input signal from around 1 mW to 1 W. In this case the amplified light was sufficiently intense and the long-wavelength portion of the Rosenbluth gain spectrum could be observed, as shown in Fig. 6. The limited gain bandwidth of the EDFA prevented measurement all the way to the short wavelength edge of the amplified spectrum.

The fluorescence could be reduced by lowering the pump intensity. Naturally, this was accompanied by a reduction of the Rosenbluth gain. Figure 7 shows the broad and relatively flat gain spectrum of a chirped grating. Its gain, however, had to be kept very low (slightly more than 5 dB) by reducing the pump intensity, otherwise the parametric fluorescence would have become too large due to the much larger gain of the noncollinear gain-guided modes. The gain spectrum of a 1.5 cm long uniform grating is shown to illustrate the bandwidth increase provided by the chirped grating (100 nm for the chirped grating compared to slightly more than 5 nm in the case of the uniform grating).

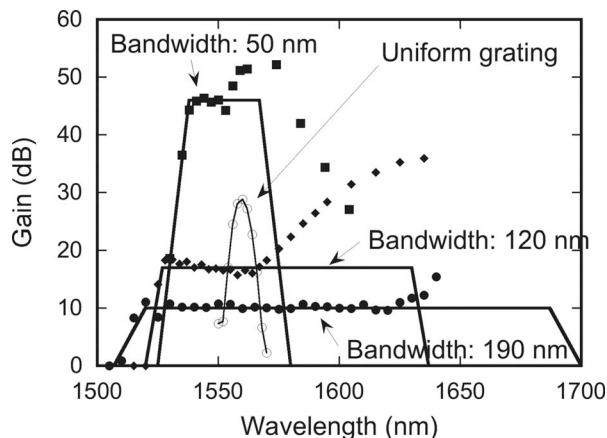


Fig. 5. Measured gain spectrum of gratings with positive chirp rate, compared to that of a shorter uniform grating. The lines are a guide to the eye.

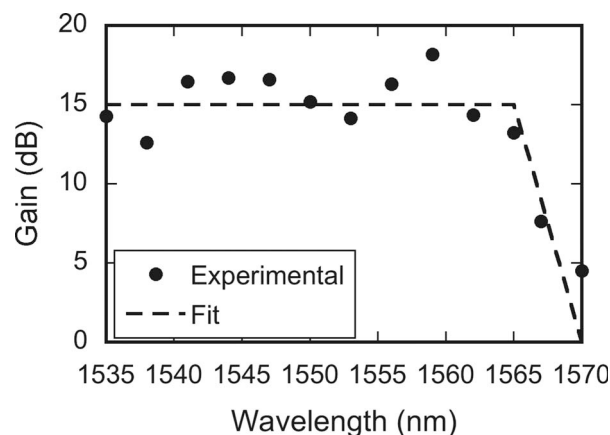


Fig. 6. Long-wavelength portion of the gain spectrum of a positively chirped grating seeded with an EDFA in order to dominate the fluorescence. The 5 cm long QPM grating was chirped in order to achieve a bandwidth of 80 nm around 1520 nm.

### B. Confirmation of the Scaling Predicted by the Rosenbluth Model

Except for the intense parametric fluorescence, the amplification spectrum of chirped gratings with positive chirp rate behaves qualitatively as predicted by the Rosenbluth model: the gain is essentially flat over a wide bandwidth. According to the Rosenbluth gain formula, Eq. (4), the logarithmic gain is proportional to the *intensity* of the pump (rather than to its amplitude) and inversely proportional to the chirp rate. Here we describe the experimental confirmation of these basic scaling laws.

We operate at a signal of 1540 nm, in the short-wavelength side of the spectrum where there is no significant parametric fluorescence, in a 5 cm long crystal, and with a pump-spot radius of  $115 \mu\text{m}$ . Figure 8(a) shows the gain as a function of pump-pulse energy for two gratings of different chirp rates. The logarithmic gain increases linearly with pulse energy (and therefore with pump intensity), as predicted by the Rosenbluth model.

Figure 8(b) shows the gain obtained with three gratings of different chirp rates at constant pump pulse en-

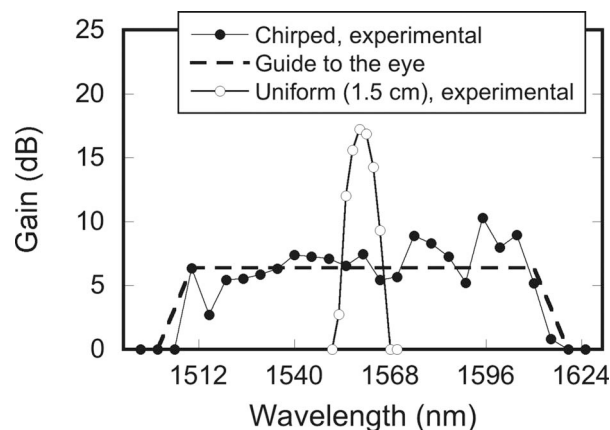


Fig. 7. Gain spectrum of a chirped QPM grating (5 cm long, designed to offer a bandwidth of 110 nm), with a pump intensity sufficiently low ( $15 \mu\text{J}$  per pulse) to cause negligible parametric fluorescence. The gain spectrum of a uniform grating is shown for comparison to illustrate the bandwidth increase due to the chirped QPM grating.

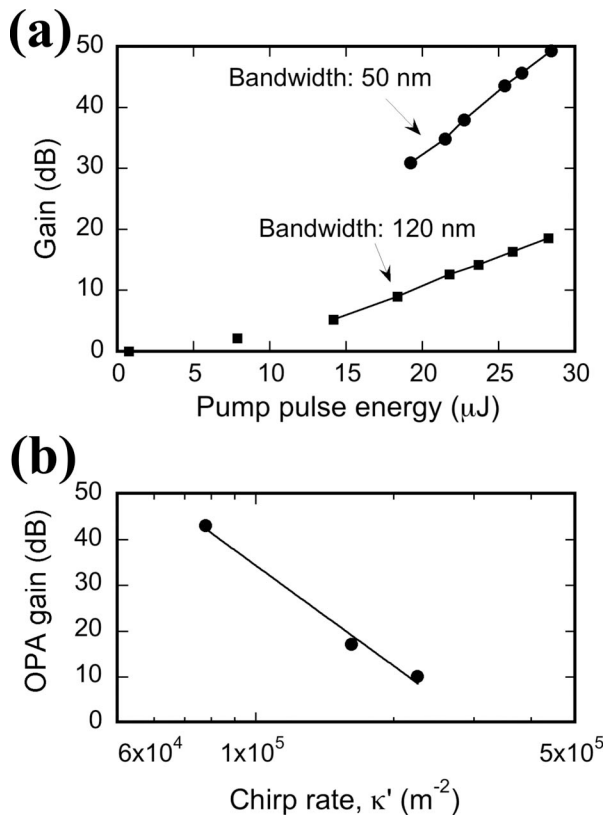


Fig. 8. (a) Gain versus pump pulse energy for two chirped gratings, measured at a signal wavelength of 1540 nm. (b) Gain versus chirp rate, measured at a signal wavelength of 1540 nm and a pump pulse energy of 25  $\mu\text{J}$ .

ergy. The linear dependence on a logarithmic scale is consistent with the fact that the Rosenbluth gain is inversely proportional to the chirp rate.

### C. Comparison with Theory

Experimental results confirmed the scaling predicted by the Rosenbluth model. To relate the absolute gain observed with the pulsed beam, Gaussian in space and time, it is necessary to suitably average the cw plane-wave result given in Eq. (4). Because the pump pulse width is long compared to group-velocity walk-off, and the focusing is looser than confocal, a good first approximation can be obtained by assuming quasi-stationary behavior in the time domain and neglecting diffraction. The resulting gain is then obtained by averaging the Rosenbluth gain over the radial and temporal profile. The expression for the gain is identical to Eq. (8), and in this case the integrated energies  $U_{\text{amplified}}$  and  $U_{\text{seed}}$  are given by

$$U_{\text{amplified}} = \int I_s(x, y, t) \exp[2\pi\gamma_0^2(x, y, t)/|\kappa'|] dx dy dt, \quad (9)$$

$$U_{\text{seed}} = \int I_s(x, y, t) dx dy dt, \quad (10)$$

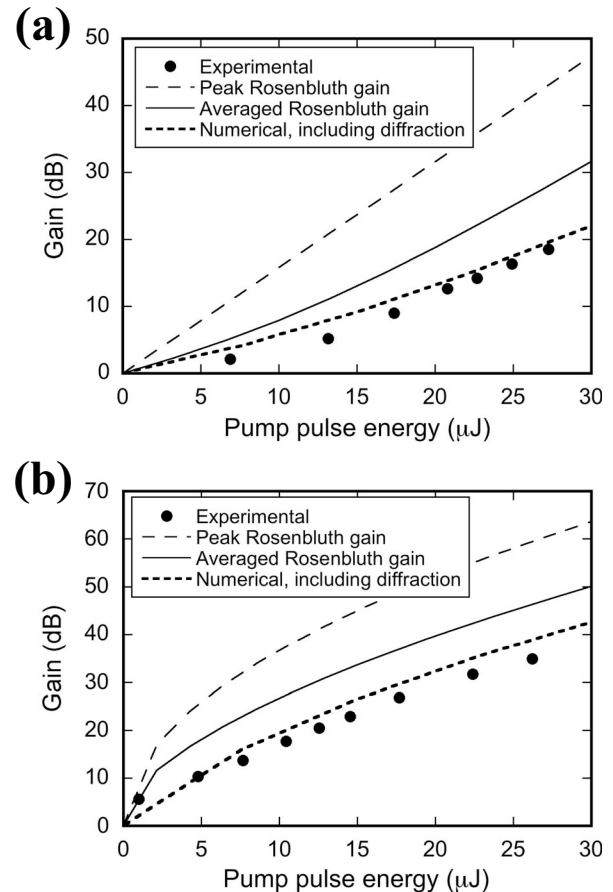


Fig. 9. Experimentally observed parametric gain, compared with theoretical values for peak and average Rosenbluth gain, as well as numerical simulations including diffraction, for (a) a 1.5 cm long uniform QPM grating and (b) a 5 cm long chirped QPM grating designed to achieve a bandwidth of 120 nm. The pump pulse energy was 25  $\mu\text{J}$ .

and it is understood that the time integrals are taken over a duration  $T_{\text{int}}$  (chosen to be longer than the pump pulse duration). In general  $I_s(x, y, t)$  is the input signal pulse and the coupling coefficient  $\gamma_0^2(x, y, t) \propto I_p(x, y, t)$  is proportional to the intensity of the pump pulse. In our experiment the input signal is cw (constant in time), so all the time dependence comes from  $\gamma_0^2(x, y, t)$ . As seen in Fig. 9 the averaged Rosenbluth formula also overestimates the gain.

Much better agreement is obtained by including diffraction into the model. In this case the coupled-mode equations must be solved numerically. We used a finite-difference beam propagator written by Schober [20]. This program includes a chirped QPM grating and diffraction, assuming radial symmetry. As shown in Fig. 9, the numerical results agree well with the experimental data.

## 5. PARASITIC NONCOLLINEAR INTERACTIONS IN NEGATIVELY CHIRPED QUASI-PHASE-MATCHED GRATINGS

As mentioned in Subsection 2.C, QPM gratings with positive and negative chirp rates behave differently in the presence of focused pump beams because of parasitic noncollinear interactions. Figure 10 illustrates this discrep-

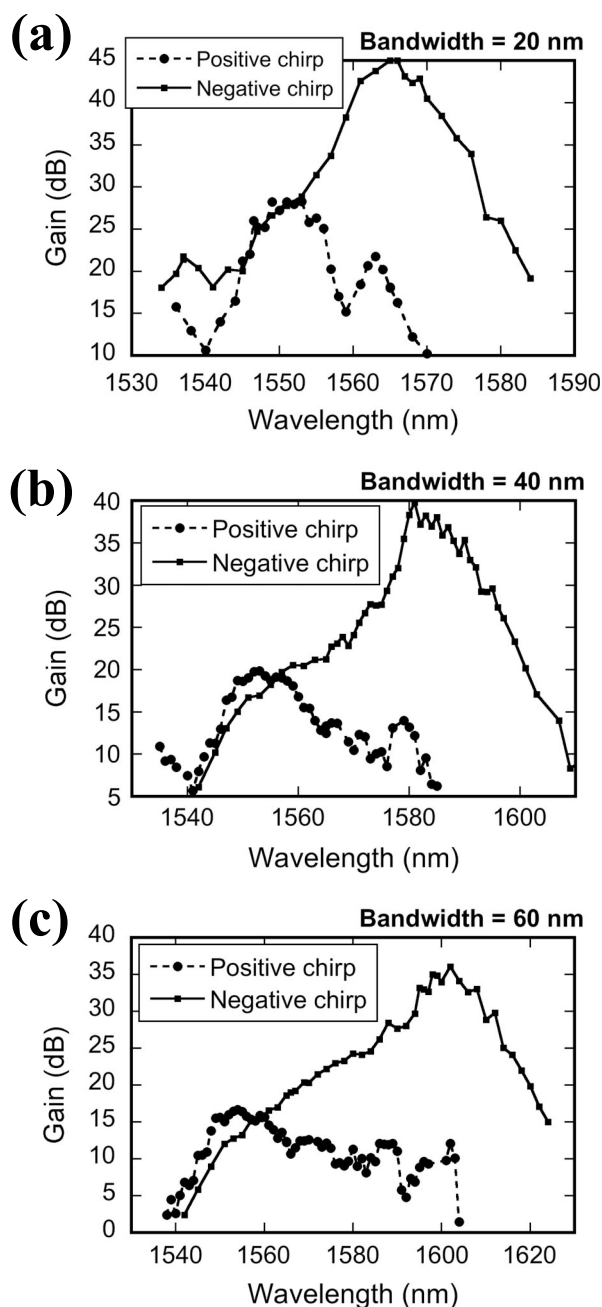


Fig. 10. Gain spectra of linearly chirped gratings with positive and negative chirp rate, seeded collinearly. The three cases correspond to chirp rates designed to phase match bandwidths of 20, 40, and 60 nm.

ancy. It shows gain spectra of linearly chirped QPM gratings with positive and negative chirp rates. In this experiment the input signal and the pump are collinear. In the case of positive chirp the gain is relatively flat over the bandwidth. However, when the chirp rate is negative the logarithmic gain varies roughly linearly across the passband.

When the chirp rate is negative, and because of the dispersion relation of lithium niobate, long wavelengths are phase matched at the *beginning* of the QPM grating. In this case parasitic noncollinear interactions enable amplification over the entire length of the grating. This is the reason why the gain is largest at long wavelengths. As the

wavelength is decreased the collinear PPMP moves towards the *output* end of the QPM grating. This shortens the amplification length and decreases the gain.

The dependence on wavelength is also visible in the far-field profile of the amplified light, shown in Fig. 11. The output has the shape of a ring, indicative of a noncollinear interaction. The bright inner ring corresponds to the amplified signal while the faint outer ring is due to parametric fluorescence. The size and intensity of the inner ring increase with wavelength, reflecting the fact that the phase-matching angle and amplification length vary across the spectrum.

Noncollinear phase matching can give rise to relatively strong parametric fluorescence. A comparison between the parametric fluorescence produced by positive and negative chirp rates is shown in Fig. 12. This grating was designed to phase-match wavelengths ranging from 1520 to 1570 nm. The measurement was taken by collecting all the emitted light (i.e., over all solid angles of significant emission). The pump energy was 25  $\mu\text{J}$  per pulse.

Figure 13 shows the far-field fluorescence patterns produced by uniform, positively chirped, and negatively chirped QPM gratings. The fluorescence patterns associated with positive chirp rates consist of two symmetric lobes, in no particular relationship with the plane of the nonlinear crystal. The reason for the two-lobe pattern is not clear; it may be related to an asymmetry in the pump beam. It differs remarkably from the ring characteristic of negative chirp rates.

## 6. NONCOLLINEAR GAIN-GUIDED MODES

### A. Experimental Setup

Noncollinear incidence angles for the signal beam were introduced using a 1 cm thick parallel glass plate placed on the path of the signal beam (but not the pump beam) prior to the focusing lens. The lateral translation of the signal beam resulting from the rotation of the plate is mapped to a noncollinear incidence angle by the focusing lens placed in front of the crystal. The pump and signal beams both lie in the plane perpendicular to the  $z$  axis of the PPLN crystal.

We used EDFAs to raise the signal power level in order to dominate the fluorescence. Two signal lasers were available for this experiment. They were both tunable ECDLs, New Focus model Vidia-Swept. Their tunable ranges were 1520–1570 and 1560–1625 nm, respectively.

The PPLN crystals were fabricated with a special phase-matching profile in order to study noncollinear modes. The beginning of each QPM grating was of a 1 cm long uniform segment used as a “pre-amplifier” to excite a noncollinear gain-guided mode. The remaining 4 cm was linearly chirped. The experiment consisted in measuring the gain provided by the nonuniform segment.

### B. Measurement of the Noncollinear Gain

The gain as a function of incidence angle is plotted in Fig. 14 for a number of uniform and chirped gratings. In the case of uniform gratings, the gain is largest at normal incidence and decreases as the angle increases. A linear fit (shown by dashed lines) to the uniform grating data was

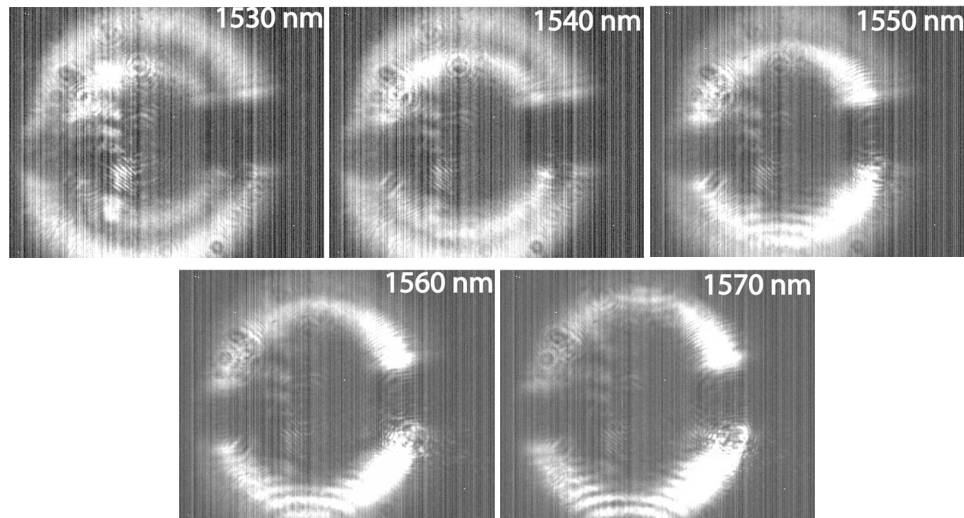


Fig. 11. Far-field pattern of the amplified signal produced by negatively chirped QPM gratings. The bright inner circle in each figure is the seeded noncollinear mode, while the weaker outer ring is the amplified parametric fluorescence. The dark line is the shadow of a wedge used to block the cw seed. The wavelength of the seed is indicated in the figure. The angle of the center of the ring for 1570 nm is approximately  $2^\circ$ .

used to remove the contribution of the uniform segment in each of the chirped gratings.

The noncollinear gain obtained in this manner is plotted on a normalized plot in order to enable comparison with theory. This plot of the normalized growth rate,  $K/\gamma_0$ , versus normalized angle,  $\sqrt{k_s/k_i}(\theta_s/\gamma_0 w_0)$ , where  $w_0$  is the half-width of the pump beam, is shown in Fig. 15 for fixed  $\kappa'/\gamma_0^2$  ratios (i.e., for fixed inverse Rosenbluth

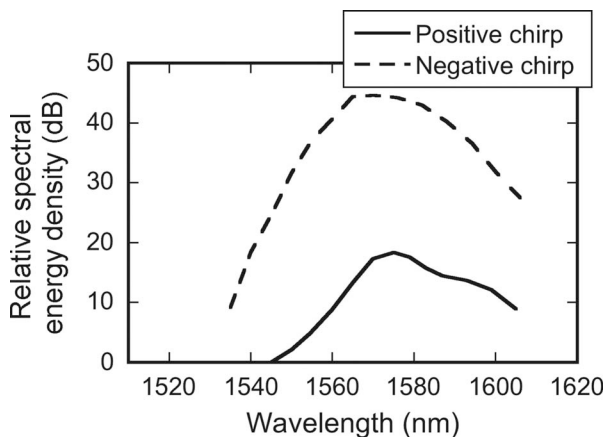


Fig. 12. Parametric fluorescence spectrum of gratings with chirp rate of equal magnitude but opposite signs. The gratings were designed to phase match wavelengths ranging from 1520 to 1570 nm. The reference level for the spectral energy density is 0.2 pJ/nm.

gain). This plot should be compared to that obtained numerically (Fig. 2). We do not expect perfect agreement because the numerical results were obtained in a 2D model while the experiment was carried out in bulk material. Nevertheless, the trends revealed by the experimental data agree with the numerical simulations. This provides an experimental demonstration of the existence of noncollinear gain-guided modes in chirped QPM OPAs.

## 7. DESIGN GUIDELINES

Before formulating design guidelines to suppress undesired noncollinear processes, let us summarize the main results concerning gain-guided modes. The growth rate  $K$  of gain-guided noncollinear modes as a function of angle was plotted in Fig. 2 for various values of the parameter  $\kappa'/\gamma_0^2 = 1/\lambda_R$ . In uniform QPM gratings the growth rate is largest in the collinear direction. On the other hand, in chirped QPM gratings gain-guided modes are suppressed in the collinear direction, but can exist over a range of noncollinear angles. For a given chirp rate, the maximum growth rate is determined only by the ratio  $\kappa'/\gamma_0^2$ . We define

$$K^*(\lambda_R) = \frac{K_{\max}}{\gamma_0}, \quad (11)$$

the ratio of the largest growth rate to the coupling coefficient. It is a function of  $\lambda_R$  only.

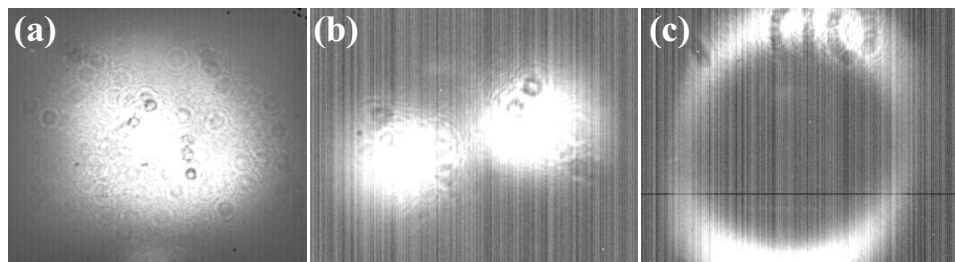


Fig. 13. Far-field parametric fluorescence patterns: (a) uniform grating, (b) positive chirp, (c) negative chirp.

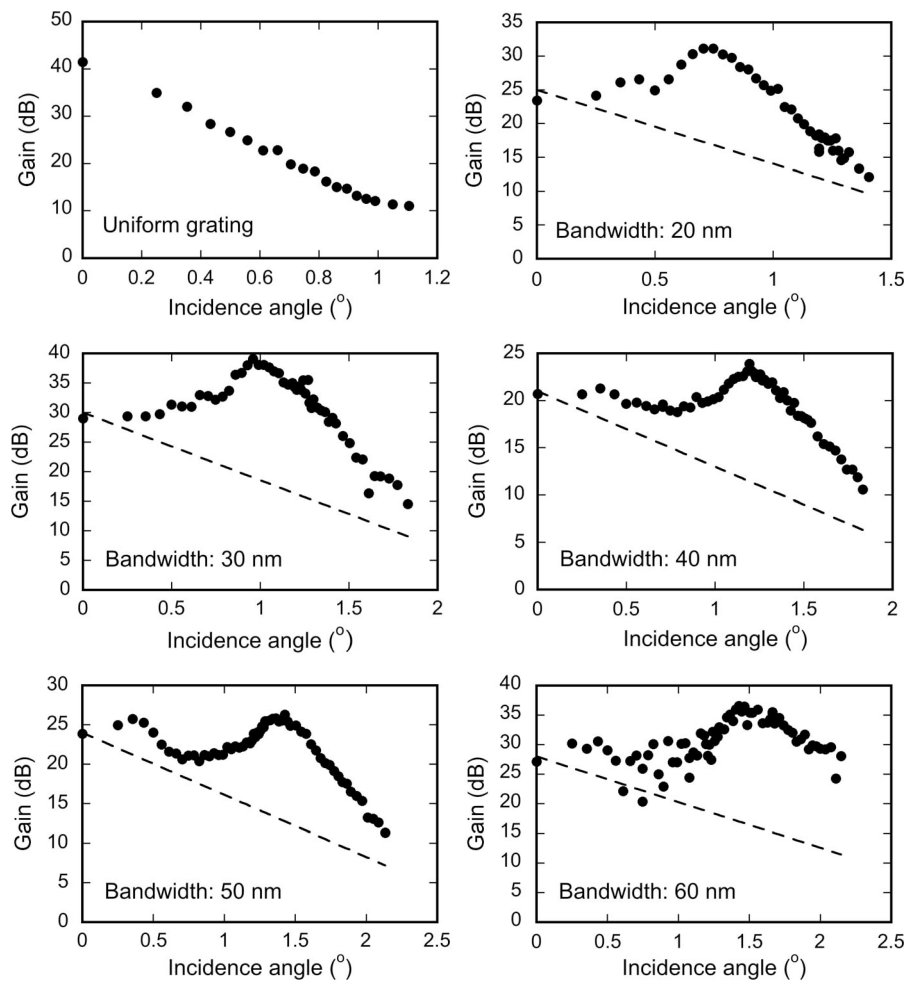


Fig. 14. Measured gain of uniform and chirped QPM gratings as a function of the incidence angle. The dashed line represents the contribution from the uniform grating segment.

Gain-guided modes are first excited around the noncollinear phase-matched point,  $z_{pm}$ , and they are amplified over the remaining length of the device if the chirp rate is negative, or until the collinear phase-matched point,  $z_{pm0}$ , if the chirp rate is positive. Therefore their gain (in the

high-gain limit) is  $G_{NC} = \frac{1}{4} \exp(2KL_{\text{gain}})$ , where the gain length is  $L_{\text{gain}} = L - z_{pm}$  if  $\kappa' < 0$  or  $L_{\text{gain}} = \min(z_{pm0} - z_{pm}, L - z_{pm})$  if  $\kappa' > 0$ . For simplicity, we will assume that the gain length is limited by the length of the grating.

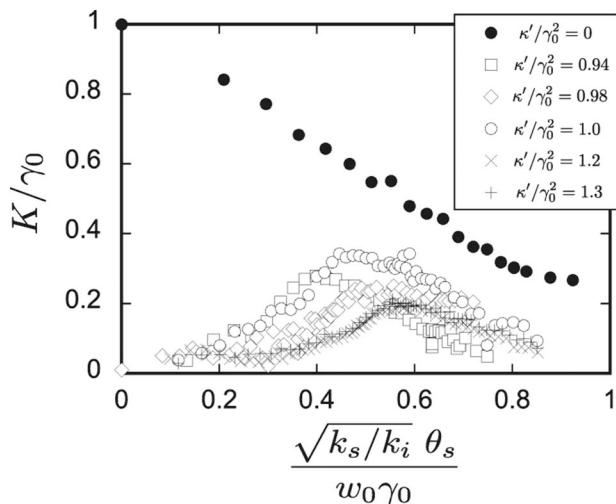


Fig. 15. Normalized growth rate,  $K/\gamma_0$ , versus normalized angle,  $\theta_s \sqrt{k_s/k_i} / \gamma_0 w_0$ , for various values of  $\kappa'/\gamma_0^2$ , with  $k_s/k_i \approx 2.1$ . Data are replotted from Fig. 14.

### A. Suppression of Parametric Fluorescence

Since they can be amplified over long distances, the gain of noncollinear modes can be much larger than the collinear gain, even though the growth rate (i.e., gain per unit length) is smaller than for the collinear case. For this reason, when seeded by parametric noise they can give rise to intense parametric fluorescence, which can spoil the contrast of the amplifier and even take energy away from the pump. It is often necessary to keep the fluorescence level much lower than the desired (useful) output power of the amplifier. This can be accomplished by using a sufficiently intense input signal, short QPM gratings, or wide pump beams (which enables spatial or spectral filtering).

Using a large enough input signal power is one way of ensuring that the parametric fluorescence is negligible compared to the amplified power. Let us obtain an estimate for the power of the parametric noise. Following [21], we assume an input intensity of one photon per mode,

$$d^2I_{in} = \frac{\hbar \omega_{s0}^3 n_{s0}^2}{4\pi^2 c^2} \theta d\theta d\omega. \quad (12)$$

The power gain seen by each frequency component is approximately  $G^2(\theta, \omega) = \frac{1}{4} \exp[2K(\theta)L_{\text{eff}}(\omega)]$ , where  $K(\theta)$  is the noncollinear growth rate and  $L_{\text{eff}}(\omega)$  is the effective gain length. This length depends on the position of the phase-matching point, which is itself a function of frequency, and can be expressed as  $L_{\text{eff}} \approx L \delta\omega / \Delta\omega_{BW}$ , where it is understood that  $\delta\omega$  is equal to zero on one side of the amplification bandwidth and to  $\Delta\omega_{BW}$  on the other side. Integrating the amplified intensity over all angles and frequencies, and multiplying by the beam area  $\pi w_0^2$ , we obtain the following approximation for the parametric noise:

$$\begin{aligned} P_{\text{out}} &\approx \frac{\hbar \omega_{s0}^3 n_{s0}^2 \pi w_0^2}{16\pi^2 c^2} \int_{\theta_{\min}}^{\theta_{\max}} \int_0^{\Delta\omega_{BW}} \exp\left[\frac{2K(\theta)L \delta\omega}{\Delta\omega_{BW}}\right] \theta d\delta\omega d\theta, \\ &\approx \frac{\hbar \omega_{s0}^3 n_{s0}^2 \pi w_0^2}{16\pi^2 c^2} \int_{\theta_{\min}}^{\theta_{\max}} \frac{\Delta\omega_{BW}}{2K(\theta)L} e^{2K(\theta)L} d\theta, \\ &\approx \frac{\hbar \omega_{s0}^3 n_{s0}^2 \pi w_0^2 \Delta\omega_{BW} \theta_{\max} \Delta\theta}{16\pi^2 c^2 \cdot 2K_{\max} L} e^{2K_{\max} L}, \\ &= \frac{1}{4} P_{\text{noise}} e^{2K_{\max} L}, \end{aligned} \quad (13)$$

where the equivalent input noise power is

$$P_{\text{noise}} \approx \frac{\hbar \omega_{s0}^3 n_{s0}^2 \pi w_0^2 \theta_{\max} \Delta\theta \Delta\omega_{BW}}{4\pi^2 c^2 \cdot 2K_{\max} L}. \quad (14)$$

In this calculation, the  $\omega$  integral was evaluated in the large-gain limit, and the  $\theta$  integral was estimated by assuming a maximum gain  $K_{\max}$  around  $\theta_{\max}$ , with an angular range of  $\Delta\theta$ .

Expression (13) means that the parametric noise is dominated by the noncollinear modes that are amplified over the entire length of the device. Typically, the equivalent input noise power  $P_{\text{noise}}$  is of the order of nanowatts over a bandwidth of a few tens of nanometers and an angular range of a few degrees. The input signal power required for the collinear gain to dominate the parametric fluorescence is thus given by

$$P_{\text{input}} \gg P_{\text{noise}} \frac{G_{NC,\max}}{G_R}, \quad (15)$$

where  $G_{NC,\max} = \frac{1}{4} \exp(2K_{\max}L)$  is the maximum power gain of the noncollinear modes and  $G_R$  is the Rosenbluth gain, given by Eq. (4).

As an example, let us consider a design of a chirped QPM OPA in LiNbO<sub>3</sub>, providing a collinear gain of 40 dB over a bandwidth of 100 nm around 1550 nm, similar to those fabricated for this experiment. For a grating length  $L = 5$  cm the desired bandwidth is achieved with a chirp rate  $\kappa' = 4.1 \times 10^5 \text{ m}^{-2}$ . The Rosenbluth gain parameter required to obtain a gain of 40 dB is  $\lambda_R \approx 1.5$ . This corresponds to a coupling coefficient of  $\gamma_0 \approx 780 \text{ m}^{-1}$ . According

to Fig. 2 the maximum growth rate of noncollinear modes is  $K_{\max} \approx 0.3 \times \gamma_0 = 233 \text{ m}^{-1}$ , leading to a noncollinear gain of  $G_{NC} \approx 3 \times 10^9$ . Assuming an equivalent noise input of  $P_{\text{noise}} \sim 10 \text{ nW}$ , we find that the amplified noise would equal the amplified signal for an input power of 3 mW.

If the available input power is insufficient to achieve a desired contrast ratio it may be necessary to design the amplifier in order to reduce the intensity of the parametric fluorescence. This can be done by decreasing the length of the QPM grating while increasing the chirp rate in order to maintain a fixed gain bandwidth. The corresponding increase in pump power required to maintain a certain gain is given by Eq. (6). As long as this relationship is maintained, the collinear (Rosenbluth) gain remains constant but the noncollinear gain is reduced. Using Eq. (11), we can rewrite the noncollinear gain as  $G_{NC,\max} = \frac{1}{4} \exp[2K^*(\lambda_R) \gamma_0 L]$ , or, using Eq. (6),

$$G_{NC,\max} = \frac{1}{4} \exp[2K^*(\lambda_R) \sqrt{\lambda_R \Delta K_g L}]. \quad (16)$$

Since all other quantities are kept constant the noncollinear gain can be reduced by decreasing the length of the QPM grating.

Again, we consider a numerical example. Let us assume that for a certain amplifier design with a grating length of 5 cm, the fastest-growing noncollinear mode has a gain of 100 dB. Now we suppose that the grating length is reduced by half, but the chirp rate and the pump power are increased in order to keep the bandwidth and the Rosenbluth gain parameter  $\lambda_R$  constant. For this new design the maximum noncollinear gain would be 70 dB: a reduction of 30 dB with respect to the original design.

An alternative way of eliminating the parametric fluorescence is to use a sufficiently wide pump beam. It is assumed that the energy of the beam is increased so as to keep the intensity, and therefore the coupling coefficient  $\gamma_0$ , constant. According to Fig. 2 the angle of noncollinear emission depends on the normalized parameter  $\bar{\theta} \propto \theta / \gamma_0 w_0$ . Therefore, the physical angle,  $\theta \propto \theta \gamma_0 w_0$ , increases with the size of the pump beam. This opens the possibility of spatially filtering the noncollinear emission. Moreover, noncollinear phase matching is accompanied by a wavelength shift with respect to the collinear gain. Consequently, parametric fluorescence is emitted at a wavelength different than that of the collinearly amplified light. By choosing the pump beam width large enough, the angle of parametric emission can be increased, and its wavelengths shifted away from the operation range of the amplifier, where spectral filtering can be used.

## B. Negatively Chirped Quasi-Phase-Matched Gratings

Noncollinear gain-guided modes can be excited by the collinear input beam itself when the chirp rate is negative. Because of the finite width of the pump beam the input signal and idler beams amplified collinearly are transversely localized and as a consequence can contain high spatial frequencies, which can seed noncollinear gain-guided modes. These modes are then amplified over the remaining length of the device. This mechanism occurs only in negatively chirped QPM gratings because they en-

able noncollinear phase matching for  $z > z_{pm0}$  (see Fig. 3). This process was observed experimentally in Section 5.

Numerical simulations [16] show that there is a certain distance between the phase-matched point and the appearance of parasitic noncollinear modes, called the threshold length, and given by

$$L_{th} = \frac{k_s w_0^2}{4\lambda_R^2}. \quad (17)$$

Strictly speaking, this relation holds only in the case of a degenerate interaction. Nevertheless, it indicates that the appearance of undesired amplification can be delayed by increasing  $w_0$ , the half-width of the pump beam. By making the threshold length longer than the grating length, it is possible to suppress parasitic amplification and to obtain the desired collinear gain. This is accomplished when

$$w_0 \gg 2\lambda_R \sqrt{\frac{L}{k_s}}. \quad (18)$$

In terms of the diffraction length  $L_{diff} = \frac{1}{2}k_s w_0^2$ , this criterion becomes  $L_{diff} \gg 2\lambda_R^2 L$ .

As an example, let us consider an OPA consisting of a PPLN crystal chirped in order to provide a 100 nm bandwidth around 1550 nm. A gain of 40 dB requires  $\lambda_R = 1.46$ . For a 5 cm long grating, the pump half-width ensuring suppression of parasitic amplification is  $w_0 \gg 445 \mu\text{m}$ .

## 8. CONCLUSION

An experimental investigation of collinear and noncollinear parametric processes existing in chirped quasi-phase-matched optical parametric amplifiers (chirped QPM OPAs) was presented. The main advantage of these devices lies in their arbitrarily large amplification bandwidths (determined by the chirp rate and length of the QPM grating), achieved in a simple collinear configuration. Chirped QPM OPAs also offer the possibility of shaping the gain and group-delay spectra.

We demonstrated experimentally that the collinear gain of chirped QPM OPAs is constant over a wide bandwidth. We confirmed the scaling predicted by the Rosenbluth model, namely, that the logarithmic gain is proportional to the pump beam intensity and inversely proportional to the chirp rate of the QPM grating.

The experiment revealed the existence of noncollinear gain-guided modes. These modes were observed experimentally by seeding the amplifier at a noncollinear angle. Since they are amplified over long distances compared to the phase-matched length of the collinear interaction, their gain can be much larger than the collinear gain.

Parasitic noncollinear interactions can be seeded by spontaneous emission and give rise to an intense parametric fluorescence. Noncollinear gain-guided modes can also be excited in negatively chirped QPM gratings by high-spatial-frequency components of the amplified seed resulting from the finite width of the pump beam.

These transverse effects must be taken into account when designing chirped QPM OPAs. The intense parametric fluorescence can be mitigated by using a suffi-

ciently intense input signal, by reducing the length of the grating and by increasing the width of the pump beam. The parasitic amplification that occurs in negatively chirped QPM gratings can also be suppressed using a sufficiently wide pump beam.

Naturally, a number of other well-known issues must be taken into account when using intense laser beams, such as self-focusing, photorefractive damage, and material breakdown.

## ACKNOWLEDGMENTS

This work was sponsored by the Air Force Office of Scientific Research (AFOSR) under grants F49620-02-1-0240 and F49620-01-1-0428. M. Charbonneau-Lefort acknowledges additional support from the Natural Sciences and Engineering Research Council of Canada. The work of B. Afeyan was supported by the laser-plasma branch of the Naval Research Laboratory (NRL) and by a Department of Energy (DOE) National Nuclear Security Administration (NNSA) Stewardship Science Academic Alliances (SSAA) grant.

## REFERENCES

1. C. G. Durfee, S. Backus, M. M. Murnane, and H. C. Kapteyn, "Design and implementation of a TW-class high-average power laser system," *IEEE J. Sel. Top. Quantum Electron.* **4**, 395–406 (1988).
2. S. Backus, C. G. Durfee, M. M. Murnane, and H. C. Kapteyn, "High power ultrafast lasers," *Rev. Sci. Instrum.* **69**, 1207–1223 (1998).
3. P. Maine, D. Strickland, P. Bado, M. Pessot, and G. Mourou, "Generation of ultrahigh peak power pulses by chirped pulse amplification," *IEEE J. Quantum Electron.* **24**, 398–403 (1988).
4. A. Dubietis, G. Jonusauskas, and A. Piskarskas, "Powerful femtosecond pulse generation by chirped and stretched pulse parametric amplification in BBO crystal," *Opt. Commun.* **88**, 437–440 (1992).
5. I. N. Ross, P. Matousek, M. Towrie, A. J. Langley, and J. L. Collier, "The prospects for ultrashort pulse duration and ultrahigh intensity using optical parametric chirped pulse amplifiers," *Opt. Lett.* **144**, 125–133 (1997).
6. J. Collier, C. Hernandez-Gomez, I. N. Ross, P. Matousek, C. N. Danson, and J. Walczak, "Evaluation of an ultrabroadband high-gain amplification technique for chirped pulse amplification facilities," *Appl. Opt.* **36**, 7486–7493 (1999).
7. I. Jovanovic, B. J. Comaskey, C. A. Ebberts, R. A. Bonner, D. M. Pennington, and E. C. Morse, "Optical parametric chirped-pulse amplifier as an alternative to Ti:sapphire regenerative amplifiers," *Appl. Opt.* **41**, 2923–2929 (2002).
8. T. Kobayashi and A. Baltuska, "Sub-5-fs pulse generation from a noncollinear optical parametric amplifier," *Meas. Sci. Technol.* **13**, 1671–1682 (2002).
9. C.-W. Hsu and C. C. Yang, "Broadband infrared generation with noncollinear optical parametric processes on periodically poled LiNbO<sub>3</sub>," *Opt. Lett.* **26**, 1412–1414 (2001).
10. A. Fragemann, V. Pasiskevicius, and F. Laurell, "Broadband nondegenerate optical parametric amplification in the mid infrared with periodically poled KTiOPO<sub>4</sub>," *Opt. Lett.* **30**, 2296–2298 (2005).

11. K. L. Baker, "Single-pass gain in a chirped quasi-phase-matched optical parametric oscillator," *Appl. Phys. Lett.* **82**, 3841–3843 (2003).
12. M. Charbonneau-Lefort, M. M. Fejer, and B. Afeyan, "Tandem chirped quasi-phase-matching grating optical parametric amplifier design for simultaneous group delay and gain control," *Opt. Lett.* **30**, 634–636 (2005).
13. M. Charbonneau-Lefort, B. Afeyan, and M. M. Fejer, "Optical parametric amplifiers using chirped quasi-phase-matching gratings I: practical design formulas," *J. Opt. Soc. Am. B* **25**, 463–480 (2008).
14. M. Charbonneau-Lefort, B. Afeyan, and M. M. Fejer, "Optical parametric amplifiers using chirped quasi-phase-matching gratings II: space-time evolution of light pulses," *J. Opt. Soc. Am. B* **25**, 683–700 (2008).
15. M. M. Fejer, G. A. Magel, D. H. Jundt, and R. L. Byer, "Quasi-phase-matched second harmonic generation: tuning and tolerances," *IEEE J. Quantum Electron.* **28**, 2631–2654 (1992).
16. M. Charbonneau-Lefort, "Optical parametric amplifiers using chirped quasi-phase-matching gratings," Ph.D. dissertation (Stanford University, 2007).
17. M. N. Rosenbluth, "Parametric instabilities in inhomogeneous media," *Phys. Rev. Lett.* **29**, 565–567 (1972).
18. J. Huang, X. P. Xie, C. Langrock, R. V. Roussev, D. S. Hum, and M. M. Fejer, "Amplitude modulation and apodization of quasi-phase-matched interactions," *Opt. Lett.* **31**, 604–606 (2006).
19. M. M. Sushchik and G. I. Freidman, "The effect of nonuniformity of the amplitude and phase distribution of the pumping radiation on the spatial locking of parametrically amplified waves," *Radiophys. Quantum Electron.* **13**, 1043–1047 (1970).
20. A. M. Schober, "Parametric interactions of short optical pulses in quasi-phase-matched nonlinear devices," Ph.D. dissertation (Stanford University, 2005).
21. R. L. Byer and S. E. Harris, "Power and bandwidth of spontaneous parametric emission," *Phys. Rev.* **168**, 1064–1068 (1968).